



ISSN: 0976-3031

Available Online at <http://www.recentscientific.com>

CODEN: IJRSFP (USA)

International Journal of Recent Scientific Research
Vol. 9, Issue, 2(C), pp. 23953-23963, February, 2018

**International Journal of
Recent Scientific
Research**

DOI: 10.24327/IJRSR

Research Article

A DESIGN FOR SUSTAINABLE TECHNOLOGY AND ADSORPTION STUDIES ON REMOVAL OF MALACHITE GREEN FROM WATER USING NUTRACEUTICAL INDUSTRIAL FENNEL SEED SPENT

Razia Sulthana and Akheel Ahmed Syed*

Department of Studies in Chemistry, University of Mysore, Manasa Gangotri,
Mysuru -570006, India

DOI: <http://dx.doi.org/10.24327/ijrsr.2018.0902.1569>

ARTICLE INFO

Article History:

Received 05th November, 2017

Received in revised form 08th

December, 2017

Accepted 10th January, 2018

Published online 28st February, 2018

Key Words:

Nutraceutical industrial fennel seed spent;
Malachite green; Adsorption isotherms

ABSTRACT

The present study explores the process of adsorption by Nutraceutical Industrial Fennel Seed Spent (NIFSS), a byproduct of Nutraceutical Industry, for the removal of Malachite Green (MG), a toxic cationic dye. In this process, the effect of various factors like initial dye concentration, adsorbent dosage, temperature, pH and particle size were studied. The experimental equilibrium data were analyzed using Langmuir, Freundlich and Tempkin isotherms. The adsorption kinetics of pseudo-first order, pseudo-second order models were used for the kinetic studies. The value of maximum adsorption capacity ($q_m = 103.09$ mg/g) was close to the experimental value ($q_e = 98.0$ mg/g), and correlation coefficient (R^2) of 0.964. The experimental data fitted very well to pseudo-second order kinetic model. The values of thermodynamic parameters like ΔG^0 , ΔH^0 and ΔS^0 indicated that adsorption was almost spontaneous and endothermic in nature. The low value of ΔH^0 suggests that the process is predominantly a physical one. From the Fourier-transform Infrared Spectroscopy (FTIR) spectra and scanning electron microscopy (SEM) images, it was apparent that MG is adsorbed onto NIFSS. Possible mechanisms of interaction that occur in MG-NIFSS system are discussed. Experimental results suggest that NIFSS is a fast and effective adsorbent for removing MG from aqueous solutions.

Copyright © Razia Sulthana and Akheel Ahmed Syed, 2018, this is an open-access article distributed under the terms of the Creative Commons Attribution License, which permits unrestricted use, distribution and reproduction in any medium, provided the original work is properly cited.

INTRODUCTION

One of the major problems concerning textile industries, which accounts for the consumption of two-third of dyes production, is the disposal of colored waste water which contains a variety of organic compounds, dyes and toxic substances. The colored waste stream disturbs the aesthetic nature, and interferes with the transmission of sunlight which hinders the photosynthetic activity. Removal of dyes by conventional waste treatment methods is difficult as they are stable to light and oxidizing agents and resistant to bacteria (Gupta *et al.*, 1997). Methods reported in the literature for removal, degradation and/or detoxification of dyes are unsatisfactory for one reason or the other. The reported methods are broadly classified as; i) biological, ii) chemical, iii) electrochemical, iv) photochemical and v) physical. These methods are selective, expensive, require dedicated infrastructure and produce copious amounts of waste. Amongst the physical methods, adsorption is considered as an efficient process because of its simplicity in operation, eco-friendly and low-cost of operation.

Adsorption on activated carbons has been proven to be very effective in removing dyes from aqueous solutions. However, exorbitant cost is the serious limitation. Currently the research is focused on the development of low-cost adsorbent. Large varieties of low cost adsorbents used for adsorption include natural, agricultural, and industrial by product and/or waste (Hameed & Khaiary, 2008). Development of economical and eco-friendly adsorbents for dye removal from aqueous solution is of paramount importance. Thus, attempts were made in this study to develop inexpensive and ecofriendly spent obtained from nutraceutical industries for the removal of dye from aqueous solutions. The nutraceutical industrial spent (NIS) generated has no manurial, fertilizer and/or feed value since it underwent thermal, mechanical and chemical processes. Thus, disposal of large amounts of waste/spent generated by nutraceutical industries is a herculean task. Presently, it is used as a fuel in boilers. Due to porous structure, it shows low calorific value which enhances the carbon foot print.

*Corresponding author: Akheel Ahmed Syed

Department of Studies in Chemistry, University of Mysore, Manasa Gangotri, Mysuru -570006, India

Nutraceutical industrial sector, is one of the leading sectors in the US and Asia-Pacific regions and its market is estimated to rise to US\$ 278.96 billion by 2021, recording a CAGR of 7.3% for the period 2015-2021 (www.pnnewswire.com 2015). Though there are no official estimates on the volume of renewable biomass available for processing, the rough estimate of waste/spent available may run into millions of tons per year. The spent generated in nutraceutical industries are ideal adsorbents for the remediation of dyes from textile industrial effluents. An ideal biosorbent for remediation of dyes should have the following characteristics: It should be available in abundance and cheap; it should have no or minimal other use(s) which may otherwise increase its price due to demand; it should have ready-to-use quality without any pre-chemical treatment; and it should have pore structure which permits better adsorption.

Fennel (*Foeniculum vulgare*) is an herbaceous plant, reaches up to 2 m height belongs to the family *Umbelliferae*. India is the largest producer of fennel seed with a production of 11×10^4 tons per year (Bhattacharya & Sharma 2004) and it is a rich source of dietary fiber. Fennel contains 1-3% volatile oil (<http://www.spices.res.in/spices/fennel.php>); and has a wide variety of vitamins, minerals, essential oil compounds, fiber, protein, and antioxidants, which prevent oxidative stress damage and strengthen the immune system. Extraction of principle component(s) from fennel leaves behind a large amount of spent which is used in the present study as a cheap and biodegradable adsorbent in the present study.

Our research school is the first to report the use of NIS as filler material in the fabrication of thermoplastic and thermoset composites and as effective adsorbents for remediation of Congo red, methylene blue and ethidium bromide dyes (Taqi *et al.*, 2017, Papegowda & Syed 2017 and Sulthana *et al.*, 2017). Despite thousands of research papers have been reported on the use of low-cost agriculture waste as biosorbent for the remediation of waste, a very little information is available on the use of dye adsorbed biosorbent commonly known as "sludge".

In continuance, we are reporting the use of NIFSS as a potential and low-cost biosorbent to remove toxic and cationic MG dye from aqueous solution and industrial effluents. The proposed template can be extended as a sustainable technology to treat effluents of textile industry as the process is simple, economical and eco-friendly. Being a sustainable technology it will make an impact on the economic viability and social relevance to address the environmental aspects of human society as the resultant sludge finds use as filler material for the fabrication of thermoplastic and thermoset composites as demonstrated by our research school (Pashaei *et al.*, 2011; Syed & Syed 2016; Syed & Syed 2016a; Syed & Syed 2012; Syed *et al.*, 2011; Syed *et al.*, 2010; Syed *et al.*, 2010a; Syed *et al.*, 2009).

Malachite green belongs to the class of triphenylmethane (TPM) dyes, widely used for the dyeing of leather, wool and silk, distilleries, jute, paper, as a food-coloring agent, food additive, in medical disinfectant and fish industries (Kumar *et al.*, 2005; Gupta *et al.*, 2004; Culp & Beland 1996; Velmurugan *et al.*, 2011). However, it is highly cytotoxic and carcinogenic to mammalian cells and acts as a liver tumor

promoter. It decreases food intake capacity, growth and fertility rates in human beings. It causes damage to liver, spleen, kidney and heart; inflicts lesions on skin, eyes, lungs, and bones (Chowdhury *et al.*, 2011). Therefore, effective treatment should be done prior to discharge into water bodies. The objectives of our present study were to investigate the potential and effectiveness of NIFSS as a low cost adsorbent for the removal of MG from aqueous solutions and design of a template for sustainable technology.

MATERIALS AND METHODS

Adsorbate preparation

Malachite green oxalate, CI. Basic green 4, [M.F. = $C_{25}H_{54}N_4O_2$, M.W. = 927.00, λ_{max} = 618 nm] was procured from sigma Aldrich Private Ltd, Mumbai, India. A stock dye solution of 1000 mg/L was prepared by dissolving required amount of dye in double distilled water. The experimental solution of desired concentration was obtained by successive dilution of stock solution. A number of standards were also prepared from the stock solution and calibration curve was drawn by measuring the absorbance at 618 nm of the solution. The molecular structure of the MG is illustrated in Figure 1.

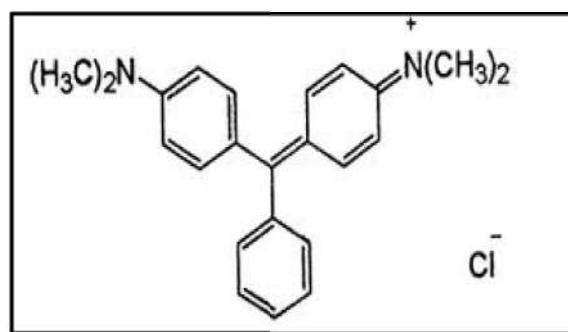


Figure 1 Structure of Malachite green

Adsorbent preparation

Nutraceutical Industrial Fennel seed spent (NIFSS) used in this study was procured from local industry. The material was dried in an oven at 60⁰ C for 24 h. The dried spent material was ground to fine powder and sieved through ASTM 80 mesh to obtain particle size of $\leq 177 \mu\text{m}$, and stored in the plastic bottles for later use. No other chemical or physical treatments were used prior to adsorption process.

Surface characterization of spent

The surface morphology of NIFSS was visualized by a Scanning Electronic Microscope (Zeiss Scanning Electron Microscope Evo/LS15, Germany). The functional groups present in the adsorbent were identified by FTIR. Infrared spectra of the NIFSS before adsorption of MG and the MG-loaded samples were obtained using a FTIR spectrometer (Inter-spec 2020, Spectro Lab, UK). Point of zero charge (pH_z) was determined to ascertain the surface charge of NIFSS.

Adsorption experiments

Adsorption of MG from aqueous solution using NIFSS was investigated by batch method. The effect of various factors

such as initial dye concentration, adsorbent dosage, temperature, pH and effect of particle size was studied. Batch adsorption experiments were carried out by adding a fixed amount of NIFSS (50mg) into 250ml Erlenmeyer flasks containing 50ml of initial dye concentration (200mg/L). The flasks were agitated in a (Kemi orbital Shaker, India) at 170 rpm at room temperature $25 \pm 2^\circ\text{C}$ for 180 min, until equilibrium was reached. Adsorbent was separated from the aqueous solution centrifuge at 8000 rpm for 10 mins, and then the concentrations were measured by a double beam UV/vis spectrophotometer (Perkin Elmer- Lambda 25, USA) at 618 nm. The adsorbed amount of MG at equilibrium $q_e(\text{mg/g})$ was calculated by using equation (1).

$$q_e = (C_0 - C_e) \frac{V}{W} \dots \dots (1)$$

Where, C_0 and C_e are concentrations (mg/L) of MG at initial and equilibrium respectively, V is solution volume (L) and W is adsorbent weight (g).

For kinetic studies, the same procedure was followed, but the aqueous samples at pre-set time intervals. The concentrations of MG were similarly measured. The amount of MG adsorbed at any time, $q_t(\text{mg/g})$, was calculated using equation (2).

$$q_t = (C_0 - C_t) \frac{V}{W} \dots \dots (2)$$

Where, C_t (mg/L) is the concentration of MG at any time. Initial concentrations of 50, and 100 mg/L of the dye and an adsorption time of 60 min (5 min intervals) were studied. For the optimum amount of adsorbent per unit mass of adsorbate, a 50 ml of dye solution was contacted with different amount of NIFSS (0.025-0.200 g/L) till equilibrium was attained.

To find out the influence of pH on dye adsorption, 50mg of NIFSS along with 50ml of dye solution of concentration 200mg/L were agitated using orbital shaker. The experiment was repeated with varying pH values ranging from 2-12. Agitation was continued for 180 min. Contact time was sufficient to reach equilibrium with constant agitation speed of 170 rpm. At equilibrium the dye concentration was measured using double beam UV/vis spectrophotometer at 618 nm. The pH was adjusted with dilute HCl and or NaOH. Solution pH was determined by pH meter (Systronics 802, India). The extent of removal of dye was determined by following equation (3).

$$\text{Dye removal \%} = \frac{(C_0 - C_e)}{C_0} \times 100 \dots \dots (3)$$

Adsorption isotherms and kinetics

Adsorption isotherms describe the interaction between the adsorbate and the adsorbent in any system. The results of different parameters as applied under different models provide information about the interaction mechanisms, surface properties and affinities of the adsorbent. The controlling of the adsorption process was determined by fitting experimental data with pseudo-first-order and pseudo-second-order kinetics. The controlling mechanism of the adsorption process was found by fitting the experimental data with the appropriate kinetic equation.

Thermodynamic parameters

Energy and entropy of a process help to understand feasibility and mechanism of the adsorption process. In the present study, thermodynamic parameters, including standard free energy (ΔG°), enthalpy change (ΔH°) and entropy change (ΔS°) were estimated by using a rate law as well as kinetic data to evaluate the extent and enthalpy of the adsorption process.

Statistical optimization by Response Surface Methodology using Central Composite design

The effects on the final adsorption capacity was described from adsorption time (A), process temperature (B), Initial dye concentration (C), adsorbent dosage (D) and pH (E). A standard experimental design was set up with 5 factors at 2 levels Table 1. ANOVA was conducted and a general quadratic regression equation was obtained. Using this equation optimization was done based on the central composite design. Surface and contour plots indicated the effect of individual as well as interaction between parameters on the adsorption capacity.

Table 1 Experimental design of high and low levels of different factors studied

Factor	Name	Units	Minimum	Maximum
A	TIME	min	0	180
B	Temperature	$^\circ\text{C}$	27	50
C	Concentration	mg/L	25	500
D	Absorbent dosage	g/L	0.025	0.2
E	pH		2	12

RESULTS AND DISCUSSION

Surface characterization of spent

Scanning Electron Microscopy

SEM was used to study the NIFSS morphology prior to MG adsorption and after MG adsorption. SEM images show the texture and porous structure of NIFSS which enhances the adsorption of dye as shown in Figure 2a.

The SEM image show of the NIFSS after adsorption where all the pores and void between the spaces have covered by the dye adsorbed on its surface Figure 2b.

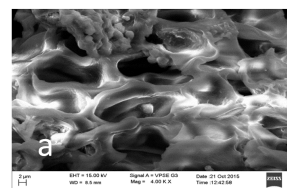


Figure 2a SEM image of NIFSS before adsorption.

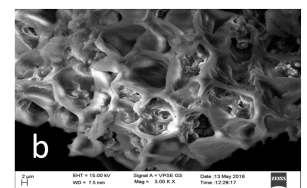


Figure 2b SEM image of NIFSS after adsorption.

FTIR Spectroscopy

The FTIR spectroscopy was employed to analyze the possible interaction between NIFSS and MG. The FTIR Spectra were recorded before and after adsorption of MG on NIFSS to determine the vibrational frequency changes for the functional groups in the adsorbent. Changes in the intensity and shift in position of the peaks were observed in the spectra after MG adsorption on NIFSS Figure 3.

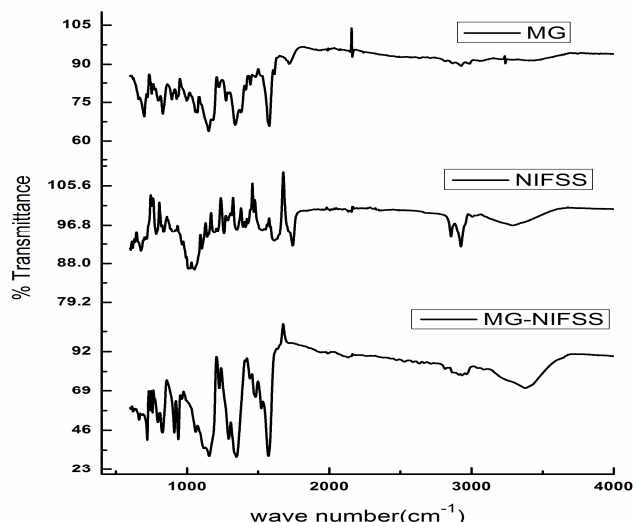


Figure 3 FTIR spectra of MG and NIFSS before and after adsorption.

The broad band around 32845 cm^{-1} was attributed to the surface hydroxyl groups, linked in cellulose and adsorbed water (Haris and Sathisviam 2009), bands at 2925 cm^{-1} 2855 cm^{-1} are due to the stretching vibrations of $-\text{CH}$ bonds in alkane and alkyl groups. Whereas, band at 1616 cm^{-1} was due to $\text{C}=\text{C}$ stretching of olefins. The band at 1411 cm^{-1} indicates methyl groups. The band at 1104 cm^{-1} was due to the presence of cellulose present in adsorbent After adsorption, increase in the band at 3377 cm^{-1} of hydroxyl group confirms that MG adsorption on NIFSS. Band at 2925 cm^{-1} is shifted to 2932 cm^{-1} corresponds to C-H stretching in methyl and methylene, where carbon is bonded with hydrogen bonds and the band at 1616 cm^{-1} is decreased to 1523 cm^{-1} due to $\text{C}=\text{C}$ stretching. The band at 1411 has decreased to 1347 cm^{-1} after adsorption may be attributed due to CH_3 group of MG and $\text{C}_{\text{aryl}}-\text{N}$ bond (Jain & Jayaram 2010), and a band at 1482 cm^{-1} was observed for the $-\text{CH}$ stretching and for $\text{C}=\text{N}$ at 1573 cm^{-1} The band at 1104 cm^{-1} has decreased to 1061 cm^{-1} after adsorption the results suggested that some of the peaks got shifted or disappeared and new peaks were detected. These changes in the spectrum may be due to involvement of those functional groups during adsorption process. The absorption bands between 1000 cm^{-1} and 600 cm^{-1} changed after the chemical modification. These observations confirm the interaction between MG and adsorbent (Zhang *et al.*, 2011).

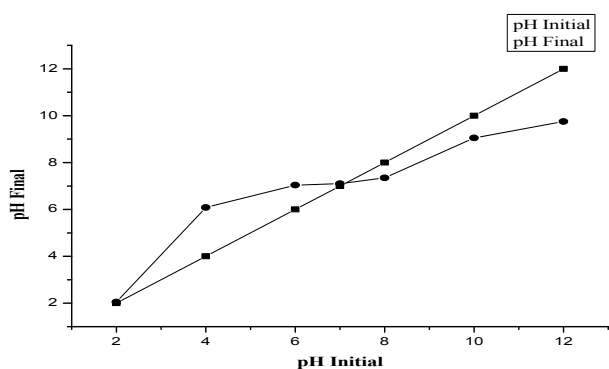


Fig 4 Point of zero charge of NIFSS

Point of Zero Charge

In order to determine Point of Zero Charge (pH_z), 0.1 M KCl was prepared, and its initial pH was adjusted between $2.0 - 12.0$ using NaOH and HCl . Then, 50 ml of 0.1 M KCl were taken in 250 ml flasks and 50 mg of NIFSS was added to each. After 24 h the final pH of the solutions was measured with a pH meter. Graphs were plotted between pH_{final} and $\text{pH}_{\text{initial}}$. Figure 4. exhibits the point of intersection of the curves at 7.1 , thus, pH_z of NIFSS is 7.1 .

Batch adsorption studies

Effect of initial dye concentration

The uptake of dye was increased from $22-190\text{ mg/g}$ respectively with the increase in dye concentration of ($25, 50, 125, 150, 175, 200, 300,$ and 500) mg/L . This may be attributed to an increase in the driving force of the concentration gradient with the increase in the initial dye concentration. The uptake of MG as a function of concentration is shown in the Figure 5a. The uptake increased with the increase in initial concentration. Initial adsorption was rapid due to the adsorption of dye onto exterior surface, after that dye molecules enter into pores (interior surface), relatively slow process. The removal of MG increased with increase in concentration and remained constant after equilibrium time.

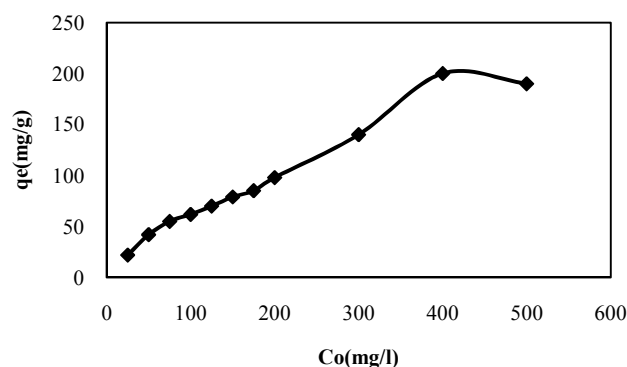


Figure 5a Effect of initial concentration of MG

Effect of adsorbent dosage

Adsorbent dosage determines the adsorption capacity of the adsorbent for a given initial concentration of the adsorbent at the operating conditions; hence it had influence on the adsorption process. The effect of adsorbent dosage on MG adsorption was investigated in the range of ($0.025-0.200\text{ g}$). It was observed that the percentage of dye removal increases with increase in adsorbent dosage. It is due to the binding of almost all dye molecules on the adsorbent surface and the establishment of equilibrium between dye molecule onto the adsorbent and in the solution (Chowdhury and Das 2012). Thus, dye sorption increased with sorbent dosage has shown in Figure 5b.

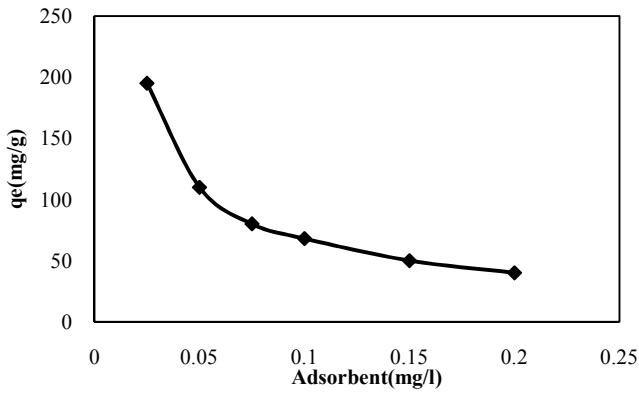


Figure 5b Effect of NIFSS on MG

Effect of Temperature

Temperature also exhibits certain influence on the adsorption process. Therefore batch adsorption experiments were carried out at different temperatures and the results are shown in Figure 5c. Adsorption capacity increased marginally, with increase in the temperature which indicates that the process was exothermic. The enhancement in adsorption with temperature may be due to the increase in the mobility of the dye molecule with increase in their kinetic energy.

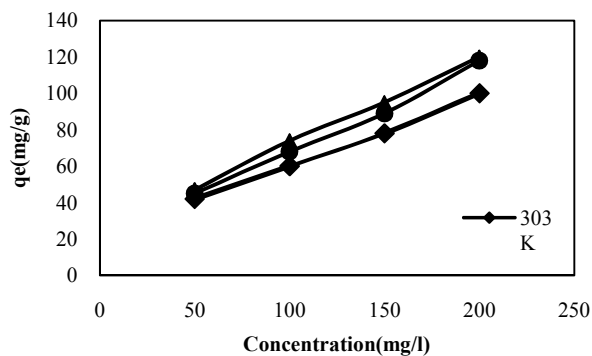


Figure 5c Effect of Temperature on MG

Effect of pH

pH is one of the most important parameters for adsorption process as it controls the adsorption capacity due to its influence on the adsorbent surface properties and ionic forms of dye in the solution (Chowdhury and Das 2012)

The adsorption capacity of spent slightly decreased with increase in solution pH and the maximum adsorption capacity for MG was observed between 4-6 pH in acidic condition. MG a cationic dye, which exists in aqueous solution as positively, charged ions. The increase in dye removal capacity at higher pH is attributed to the reduction of H^+ ion which competes with dye cation at lower pH for appropriate sites on the adsorbent surface. However with increase in pH, this competition weakens and dye cations replace H^+ ions bound to the adsorbent surface resulting in increased dye uptake. Similar observation has been reported for sorption of MG onto degreased coffee bean (Baek *et al.*, 2010) and activated carbon prepared from bamboo (Zhang *et al.*, 2011). The results are shown in Figure 5d.

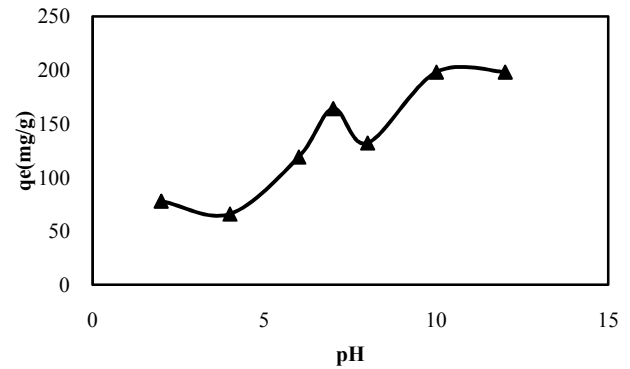


Figure 5d Effect of pH on MG

Influence of particle size

To observe the effect of particle size of adsorbents of six sized NIFSS mesh particles of ≤ 90 , ≥ 90 , ≥ 120 , ≥ 177 , ≥ 355 and ≥ 550 was studied for 200 mg/l concentrations of MG. The results of variation of these particle sizes on dye adsorption are shown in Figure 5e. It can be observed that as the particle size increases the adsorption of dye decreases and hence the percentage removal of dye also decreases. This is due to larger surface area that is associated with smaller particles. For larger particles, the diffusion resistance to mass transfer is higher and most of the internal surface of the particle may not be utilized for adsorption and consequently amount of dye adsorbed is small.

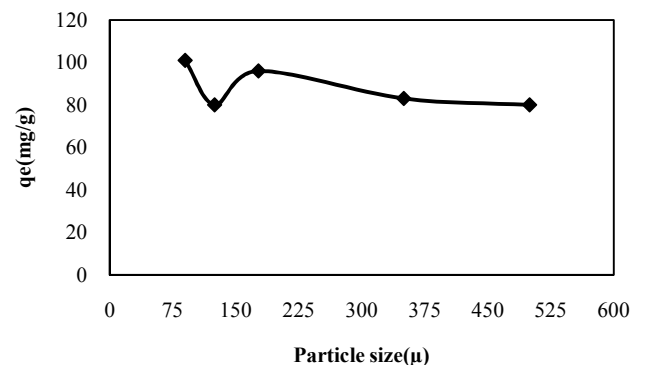


Figure 5e Effect of particle size on MG

Adsorption isotherms

Equilibrium data commonly known as adsorption isotherm describes how the adsorbate interacts with adsorbent(s) and gives a comprehensive understanding of the nature of interaction (Gupta *et al.*, 2011). Langmuir and Freundlich adsorption isotherms were used for the analysis of the MG-NIFSS adsorption system. The most common types of isotherms are Langmuir (equation 4) Freundlich (equation 5) and Tempkin (equation 6) isotherm models. of Langmuir assumes that there is monolayer adsorption on to the surface of an adsorbent containing a finite number of identical adsorption sites of uniform energy (Langmuir 1916) while Freundlich isotherm (Freundlich 1906) model is used to describe adsorption on surface having heterogeneous energy distribution and Tempkin model (Amela *et al.*, 2012) describes the process by considering some indirect adsorbate-adsorbate interactions on adsorption and the linear decrease in heat of adsorption of all the molecules and the equations are:

Langmuir isotherm: $C_e/q_e = (1/bq_{max}) + (1/q_{max})C_e$ (4)

Freundlich isotherm: $\ln q_e = \ln K_F + (1/n)\ln C_e$ (5)

Tempkin isotherm: $q_e = RT/b \ln A + RT/b \ln C_e$ where $B = RT/b$ (6)

where C_e is the concentration of dye solution at equilibrium (mg/L), q_e is the amount of dye at equilibrium in unit mass of adsorbent (mg/g), q_{max} is the monolayer adsorption capacity (mg/g) and b is the Langmuir constant (L/mg) related to the free energy of adsorption are the Langmuir coefficient related to adsorption capacity (mg/g) and adsorption energy (L/mg), respectively. K_F and n are the Freundlich coefficient related to adsorption capacity [$\text{mg/g} (\text{mg/L})^{-1/n}$] and adsorption intensity of adsorbent, A and B are Tempkin constants, related to equilibrium binding constant (L/g) and heat of adsorption (J/mol), values are calculated from intercept and slope of the linear plot respectively.

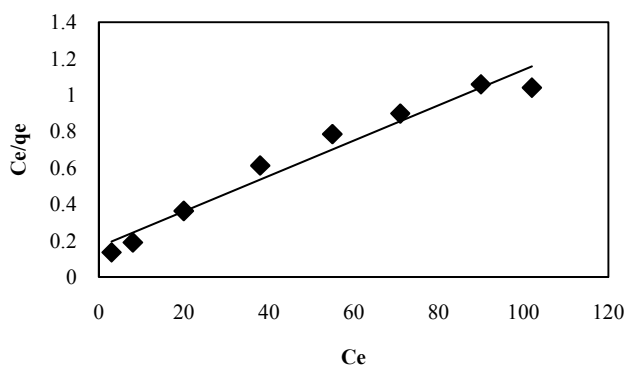


Figure 6a Langmuir adsorption isotherm model for adsorption of MG on NIFSS

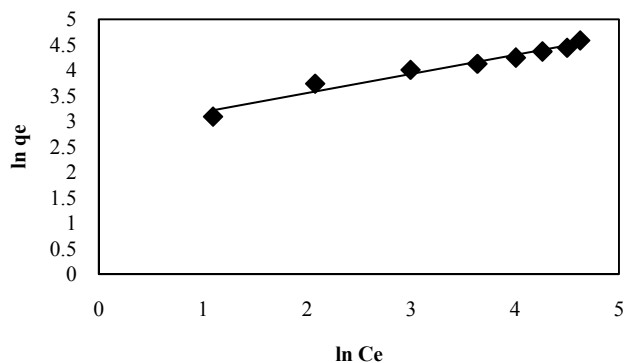


Figure 6b Freundlich adsorption isotherm model for adsorption of MG on NIFSS

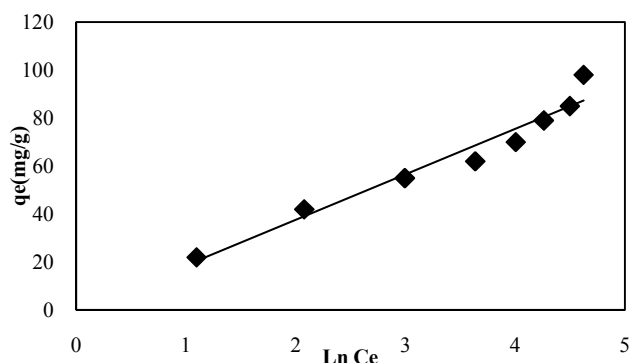


Figure 6c Tempkin adsorption isotherm model for adsorption of MG on NIFSS

Adsorption isotherms were conducted for different initial concentrations of MG in the range (25-200 mg/L). The experimental data shows a straight line with a good correlation coefficient (R^2) and q_{max} is 103 mg/g indicating more favorable adsorption of MG onto NIFSS (Figure 6a) shows that the adsorption of MG follows Langmuir isotherm.

The heterogeneity factor (n) which indicates whether the nature of adsorption is linear ($n = 1$), chemisorption ($n < 1$), or a physisorption ($n > 1$). In the present study, the value of $n = 2.678$, indicates that the adsorption is physisorption. The values of K_F and n are calculated from the intercept and slope of the plot $\ln q_e$ versus $\ln C_e$ (Figure 6b) whereas Tempkin isotherm fit well to the experimental data with R^2 value 0.951 (Figure 6c), respectively. In brief, the three models studied, namely Langmuir, Freundlich and Tempkin suggest that the interaction of MG on NIFSS is linear, favourable and physical in nature.

The Langmuir, Freundlich and Tempkin isotherm constants and regression coefficients are listed in the (Table 2).

Table 2 Isotherm Constants of MG adsorption onto NIFSS

Langmuir Constants			Freundlich Constants			Tempkin isotherm
q_{max}	b	R^2	K_F	n	R^2	A
103.09	0.058	0.963	16.543	2.678	0.964	1.019

Adsorption kinetics

Several adsorption kinetic models have been established to describe the reaction order of adsorption systems based on solution concentration, however, the pseudo-first-order and pseudo-second-order kinetic models are the most well liked models to study the adsorption kinetics and have been widely used in the most adsorption kinetic studies (Önal 2006). The controlling mechanism of the adsorption process was investigated by fitting the experimental data with pseudo-first-order; pseudo-second-order equations defined as follow:

$$\text{Pseudo-first order} \quad \log (q_e - q_t) = \log q_e - (k_1/2.303) t \quad (9)$$

$$\text{Pseudo-second order} \quad t/q_t = 1/k_2 q^2 e + t/q_e \quad (10)$$

Where k_1 and k_2 are pseudo-first order and pseudo-second order rate constants by plotting $\log (q_e - q_t)$ against Time (t) and t/q_t against time (t). The kinetic data were analysed by using different kinetic models: pseudo-first order (Ho & McKay, 1998) pseudo-second order (Lopes et al., 2003) initial MG concentrations employed during the kinetic studies were 50 and 100 ppm. These studies show a similarity when compared with other studies reported (Hameed & Khaiary 2008a; Lagergren 1898) by studying the kinetics at different temperatures (303 K, 313 K and 323 K) it was possible to understand the changes in rate of adsorption with changes in temperature. The estimated parameters are shown in (Tables 3). Based on the coefficients of determination (R^2) the pseudo-first-order model (Figures 7a & 7b.) pseudo-second order model were best fit with the experimental data for all initial MG concentrations (50 and 100 ppm) (Figures 7c & 7d). It is interesting to observe that the rate of adsorption at the very beginning of the process is very high and then slows down over time to become stagnant as it achieves the maximum adsorption. As expected the adsorption

capacity (q_e) seems to increase with increase in temperature. Consequently, based on these results, the adsorption processes were found not to be the rate-limiting step. The predictions of equilibrium adsorption capacities (q_e) were similar to pseudo-second order models and quite close to experimental values. This indicated that the kinetics of MG adsorption onto NIFSS was adherent to pseudo-second order kinetics with respect to time irrespective of the changes in initial concentration of the MG in the solution.

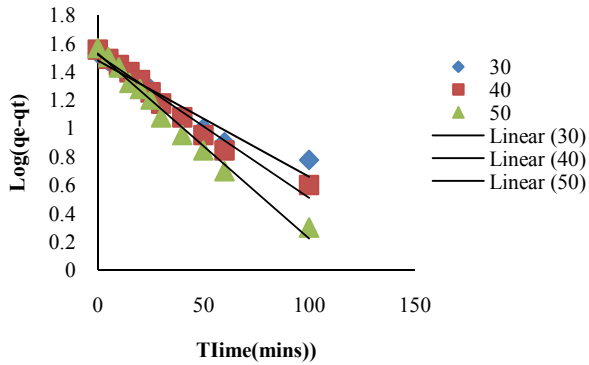


Figure 7 a pseudo-first order kinetic model fits for 50 ppm initial concentration of MG on NIFSS system at different temperatures

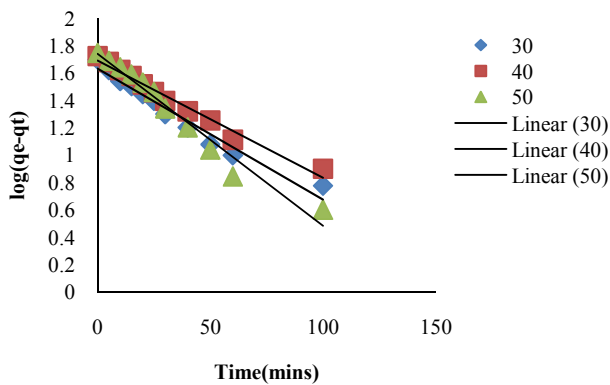


Figure 7 b pseudo-first order kinetic model fits for 100 ppm initial concentration of MG on NIFSS system at different temperatures

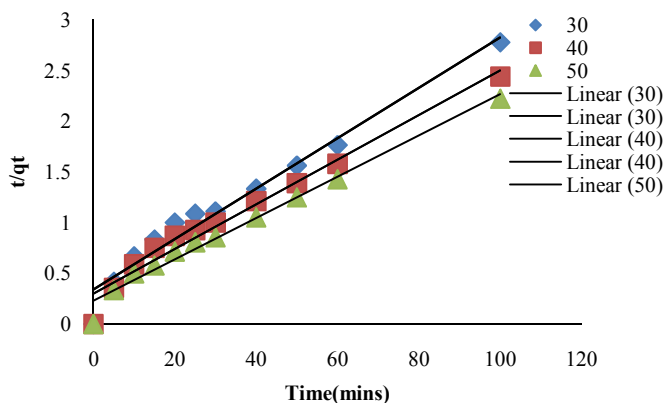


Figure 7 c pseudo-second order kinetic model fits for 50 ppm initial concentration of MG on NIFSS system at temperatures

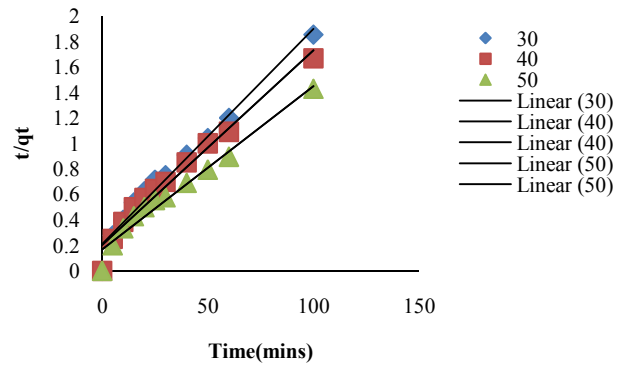


Figure 7d pseudo-second order kinetic model fits for 100 ppm initial concentration of MG on NIFSS system at different temperatures

Table 3 Experimentally determined and theoretically predicted parameters for adsorption kinetics Models

Initial Concentration [ppm]	Temp [K]	pseudo-first order(g/mg min)				pseudo-second order (g/mg min)			
		q_e^{expt} [mg.g ⁻¹]	q_e^{pred} [mg.g ⁻¹]	k_1	R^2	q_e^{pred} [mg.g ⁻¹]	k_2	R^2	
50	303	42	30.13	0.018	0.933	40.16	118.5	0.965	
	313	45	33.22	0.023	0.973	45.45	151.6	0.966	
	323	47	33.82	0.029	0.986	49.01	215.2	0.98	
100	303	54	43.07	0.022	0.963	59.17	281.89	0.973	
	313	68	42.61	0.019	0.978	65.35	322.4	0.969	
	323	74	55.24	0.029	0.966	78.12	464.4	0.966	

Effect of thermodynamic parameters

Thermodynamic parameters such as Gibbs free energy (ΔG^0), enthalpy (ΔH^0) and entropy (ΔS^0) of adsorption were calculated using the following equations:

$$\text{Log}(q_e m / C_e) = \Delta S^0 / 2.303R + (-\Delta H^0 / 2.303RT) \tag{7}$$

$$\Delta G^0 = \Delta H^0 - T\Delta S^0 \tag{8}$$

Where, m is adsorbent dose (g/L), C_e is the concentration of dye in equilibrium solution (mg/L), q_e is quantum of dye adsorbed at equilibrium in unit mass of adsorbent (mg/g), q_e/C_e is the adsorption affinity. ΔH^0 , ΔS^0 and ΔG^0 are changes in enthalpy (ΔH^0 , kJ/mol), entropy (ΔS^0 , J/mol/K) and free energy (ΔG^0 , kJ/mol) respectively; R is the gas constant (8.314/Jmol/K) and T is temperature in Kelvin. ΔH^0 and ΔS^0 values are from Van't Hoff plots of $\log(q_e m / C_e)$ vs. $1/T$, respectively. Thereafter, ΔG^0 values are obtained from equation 8.

Table 4 shows the values of thermodynamic parameters. All the values of ΔH^0 are positive which indicate the endothermic nature of adsorption and the adsorption is physical since the standard enthalpy change for a chemical reaction is normally >200 kJ/mol and the adsorption capability increases with increase in temperature. All the values of ΔS^0 are positive which suggest high MG affinity towards adsorbent and more randomness at the surface of the solid solution. All the values of ΔG^0 are negative which indicate the decrease in Gibb's free energy which verifies the feasibility and spontaneity of the adsorption process (Zhang *et al.*, 2011). The ΔG^0 value is negative for all studied temperatures. This indicates that the adsorption of MG onto NIFSS follows a spontaneous and favorable trend. The ΔG^0 value decreased with increase in temperature, indicating an increase in absorption at higher temperatures.

Table 4 Thermodynamic Parameters for MG adsorption onto NIFSS

Concentration (mg/l)	ΔH° (kJmol ⁻¹)	ΔS° (Jmol ⁻¹ K ⁻¹)	$-\Delta G^\circ$ (kJmol ⁻¹)		
			303 K	313 K	323 K
50	44.25	173.08	8.19	9.92	11.65
100	25.99	102.53	5.07	6.10	7.12
150	19.02	76.93	4.29	5.06	5.83
200	16.73	68.99	4.16	4.85	5.54

Statistical optimization by central composite design

The first step in the optimization was to determine and fit an appropriate model regression to the experimental data obtained based on a central composite design

$$\text{Biosorption} = 32.8 + 56.8 \cdot A - 0.5 \cdot B + 33.8 \cdot C - 57.0 \cdot D + 72.1 \cdot E + 48.2 \cdot AC - 5.6 \cdot BC - 21.1 \cdot A^2 + 3.3 \cdot B^2 - 37.5 \cdot C^2 + 60.0 \cdot D^2 + 22.4 \cdot E^2$$

Cross product of factors like AB AD AE etc. are zero hence excluded from the equation

The optimal values of the variables determined by maximization of the second-order polynomial equation with interaction terms obtained by multiple regression analysis based on a central composite experimental design model and the input parameters were established (Table 1) at the temperature of 40°C, pH of 11, biosorbent dosage of 0.025 g/L and initial dye concentration of 150 mg/L with adsorption time of 110 min. The predicted sorption capacity for these optimal values was 219 mg/g.

Table 5 ANOVA for central composite design

Source	Sum of Squares	Degree of freedom	Mean Square	F Value	P- Value
Model	187520.5	13	14424.7	148.17	< 0.0001**
A	6459.9	1	6459.9	66.35	< 0.0001**
B	0.6	1	0.6	0.01	0.937
C	990.3	1	990.3	10.17	0.002**
D	13027.0	1	13027.0	133.81	< 0.0001**
E	14544.0	1	14544.0	149.39	< 0.0001**
AC	2606.4	1	2606.4	26.77	< 0.0001**
BC	41.41	1	41.41	0.43	0.52
A2	3700.0	1	3699.99	38.01	< 0.0001**
B2	126.2	1	126.18	1.30	0.26
C2	3210.9	1	3210.92	32.98	< 0.0001**
D2	3349.7	1	3349.73	34.41	< 0.0001**
E2	902.7	1	902.68	9.27	< 0.0001**
Residual	8567.1	88	97.35		
Lack of fit	6095.1	86	70.87	0.06	1.00
Total	196087.6	101			

Significant figures

+ Suggestive significance (P value: 0.05 < P < 0.10)

* Moderately significant (P value: 0.01 < P ≤ 0.05)

** Strongly significant (P value: P ≤ 0.01)

	R-Squared	95.6%
Adj R-Squared		95%
Pred R-Squared		89.1%
C.V. %		17.84101

The fit of the quadratic polynomial equation to the experimental data was confirmed by both the regression coefficient, which is quite high with a value of 0.95, and the analysis of variance (ANOVA) (Table 5). The P-value for the

F-test with value 0.05 indicates that the equation is statistically significant regression model. Thus it can be successfully used in optimization of MG biosorption. The results confirm the accuracy of approximation by the quadratic equation.

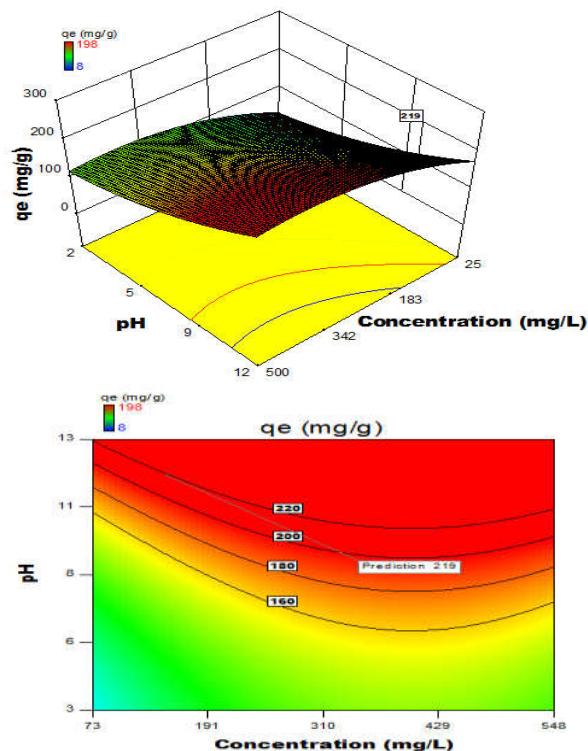


Figure 8 (a) 3D surface plot and (b) contour plot showing the variation of adsorption capacity with initial dye concentration and process pH.

The last step of the statistical optimization was the analysis of 3D response surface plots (Figure 8) as a function of two independent variables, which served the purpose of determining the interaction effects between two parameters keeping others at a fixed value (in this case the optimum value). Statistical process optimization, in a given range of parameter values, allows not only for calculating the optimal condition, but also for determining the effect of the process conditions on the biosorption. In Fig.8 it can be observed that the lower the biosorbent dosage (D) and at higher pH (E), higher is the sorption capacity (qe). The values of the regression coefficients indicate the effect of the parameter on the adsorption capacity. Positive values indicate incremental effect, for example, an increase in the initial dye concentration (C) causes a significant increase in sorption capacity. Likewise, a positive negative value indicates a detrimental effect, as seen in the case of pH (E), an increase in pH increases the adsorption capacity of the adsorbent. This is graphically represented in the surface and contour plots (Figures 8-10).

As the values of process time initial dye concentration increase there is an observable increase in absorption capacity, whereas, when considering their combined effect (i.e., for example effect of process time and process temperature on adsorption capacity) there is almost negligible effect (reflected by the coefficient value). Similarly, individually the adsorbent dosage and pH have positive values for co-efficient, indicating that as their value increases the adsorption capacity increases.

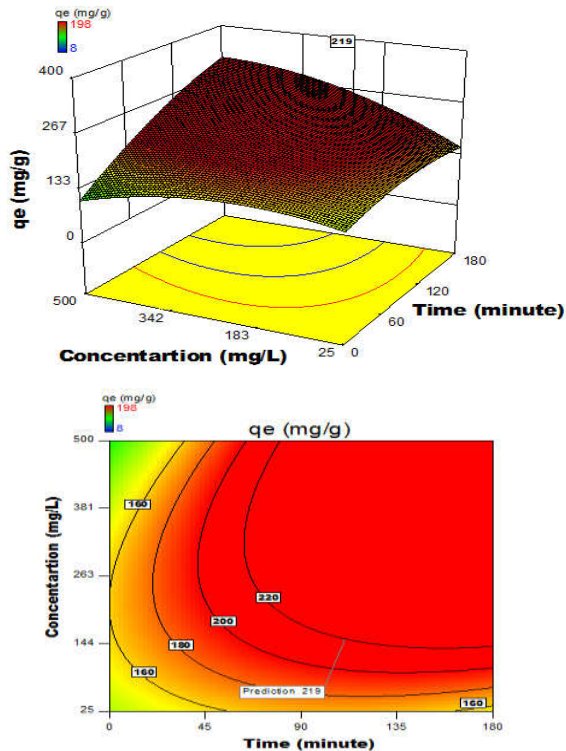


Figure 9 (a) 3D surface plot and (b) contour plot showing the variation of adsorption capacity with initial dye concentration and process time.

As the values of process time initial dye concentration increase there is an observable increase in adsorption capacity, whereas, when considering their combined effect (i.e., for example effect of process time and process temperature on adsorption capacity) there is almost negligible effect (reflected by the coefficient value). Similarly, individually the adsorbent dosage and pH have positive values for co-efficient, indicating that as their value increases the adsorption capacity increases.

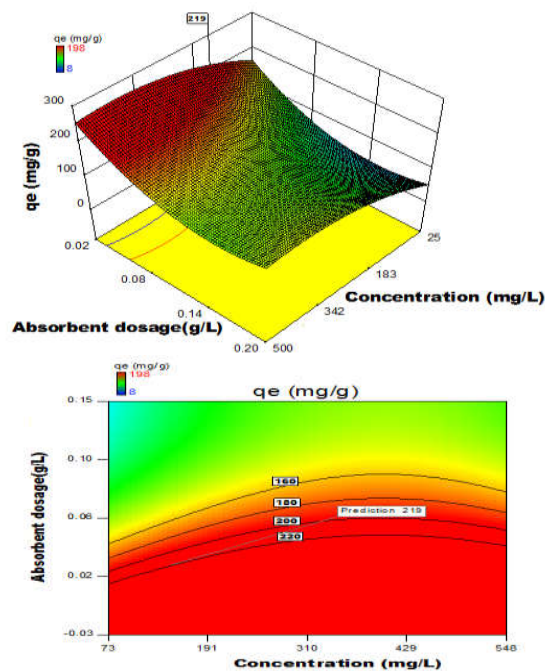


Figure 10 (a) 3D surface plot and (b) contour plot showing the variation of sorption capacity with adsorbent dose and Initial concentration.

The dependence of the sorption capacity on the initial dye concentration indicates the occurrence of a maximum of about 219 mg/L, which was confirmed by maximization of obtained quadratic polynomial expression. Increasing the initial concentration by decreasing the adsorbent dose lead to removal of a pollutant from an aqueous solution and the results reflect this.

Table 6 Optimized conditions obtained from the statistical response optimizer

Time	Temperature	Concentration	Absorbent dosage	pH	qe
110.4	40.8	149.1	0.025	11.7	219.0

The statistical significance of each operating factor was evaluated by F-test and P-values (Table 6). The F-test for testing the significance of the individual terms of the model is based on the test statistic that is calculated by dividing a regression coefficient by its variance. The results of F-test and associated P-values with confidential level >95% reveal that the most significant are A, C, D, E and AC effects, while the others seems to be unimportant.

CONCLUSION

The present study shows that NIFSS is effective biosorbent for the removal of malachite green from aqueous solution. The MG adsorption from aqueous solution by Nutraceutical Industrial Fennel seed Spent (NIFSS) is dependent on contact time, initial pH of the solution, adsorbent dose and initial MG concentration. Based on the isotherm analysis and taking into consideration the value of q_m , the adsorption data of NIFSS adsorbent is well described by Langmuir, Freundlich and Tempkin isotherm and the adsorption kinetics fitted the pseudo-second order kinetics model. The optimal values of the variables determined by maximization of the second-order polynomial equation with interaction terms obtained by multiple regression analysis done as per central composite experimental design model and the input parameters, the predicted sorption capacity of NIFSS for those optimized values was 219 mg/g. It is envisaged that cost-effective and ready-to-use NIFSS derived from nutraceutical industry for the removal of MG dye from water is not only feasible but also is a commercially challenging proposition.

Acknowledgments

One of the author (RS) gratefully acknowledges University Grants Commission, Government of India for the award of Research Fellowship for Science and Meritorious Students (RFSMS).

References

- Amela, K., Hassen, M. A., & Kerroum, D. (2012). Isotherm and kinetics study of biosorption of cationic dye onto banana peel. *Energy Procedia*, 19, 286-295.
- Baek, M. H., Ijagbemi, C. O., Se-Jin, O., & Kim, D. S. (2010). Removal of Malachite Green from aqueous solution using degreased coffee bean. *Journal of Hazardous Materials*, 176(1), 820-828.
- Bhattacharyya, K. G., & Sharma, A. (2004). Azadirachtaindica leaf powder as an effective biosorbent for dyes: a case study with aqueous Congo Red

- solutions. *Journal of Environmental Management*, 71(3), 217-229.
4. Chowdhury, S., Mishra, R., Saha, P., & Kushwaha, P. (2011). Adsorption thermodynamics, kinetics and isosteric heat of adsorption of malachite green onto chemically modified rice husk. *Desalination*, 265(1), 159-168.
 5. Chowdhury, S., & Das, P. (2012). Utilization of a domestic waste—Eggshells for removal of hazardous Malachite Green from aqueous solutions. *Environmental Progress & Sustainable Energy*, 31(3), 415-425.
 6. Culp, S. J., & Beland, F. A. (1996). Malachite green: a toxicological review. *Journal of the American College of Toxicology*, 15(3), 219-238.
 7. Freundlich, H. M. F. (1906). Over the adsorption in solution. *Journal of Physical Chemistry*, 57(385471), 1100-1107.
 8. Gupta, V. K., Srivastava, S. K., & Mohan, D. (1997). Equilibrium uptake, sorption dynamics, process optimization, and column operations for the removal and recovery of malachite green from wastewater using activated carbon and activated slag. *Industrial & engineering chemistry research*, 36(6), 2207-2218.
 9. Gupta, V. K., Mittal, A., Krishnan, L., & Gajbe, V. (2004). Adsorption kinetics and column operations for the removal and recovery of malachite green from wastewater using bottom ash. *Separation and Purification Technology*, 40(1), 87-96.
 10. Gupta, N., Kushwaha, A., & Chattopadhyaya, M. (2011). Kinetics and thermodynamics of malachite green adsorption on banana pseudo-stem fibers. *Journal of Chemical and Pharmaceutical Research*, 3(1), 284-296.
 11. Hameed, B. H., & El-Khaiary, M. I. (2008). Malachite green adsorption by rattan sawdust: Isotherm, kinetic and mechanism modeling. *Journal of Hazardous Materials*, 159(2-3), 574-579.
 12. Hameed, B. H., & El-Khaiary, M. I. (2008a). Equilibrium, kinetics and mechanism of malachite green adsorption on activated carbon prepared from bamboo by K₂CO₃ activation and subsequent gasification with CO₂. *Journal of Hazardous Materials*, 157(2), 344-351.
 13. Haris, M. R., & Sathasivam, K. (2009). The removal of methyl red from aqueous solutions using banana pseudostem fibers. *American Journal of Applied Sciences*, 6(9), 1690.
 14. Ho, Y. S., & McKay, G. (1998). Sorption of dye from aqueous solution by peat. *Chemical Engineering Journal*, 70(2), 115-124.
 15. <http://www.spices.res.in/spices/fennel.php>.
 16. Jain, S., & Jayaram, R. V. (2010). Removal of basic dyes from aqueous solution by low-cost adsorbent: Wood apple shell (*Feronia acidissima*). *Desalination*, 250(3), 921-927.
 17. Kumar, K. V., Sivanesan, S., & Ramamurthi, V. (2005). Adsorption of malachite green onto *Pithophora* sp., a fresh water algae: equilibrium and kinetic modelling. *Process Biochemistry*, 40(8), 2865-2872.
 18. Lagergren, S. K. (1898). About the theory of so-called adsorption of soluble substances. *Sven Vetenskapsakad Handlingar*, 24, 1-39.
 19. Langmuir, I. (1916). The constitution and fundamental properties of solids and liquids. Part I. Solids. *Journal of the American Chemical Society*, 38(11), 2221-2295.
 20. Lopes, E. C., dos Anjos, F. S., Vieira, E. F., & Cestari, A. R. (2003). An alternative Avrami equation to evaluate kinetic parameters of the interaction of Hg (II) with thin chitosan membranes. *Journal of Colloid and Interface Science*, 263(2), 542-547
 21. Önal, Y. (2006). Kinetics of adsorption of dyes from aqueous solution using activated carbon prepared from waste apricot. *Journal of hazardous materials*, 137(3), 1719-1728.
 22. Papegowda, P. K., & Syed, A. A. (2017). Isotherm, Kinetic and Thermodynamic Studies on the Removal of Methylene Blue Dye from Aqueous Solution Using Saw Palmetto Spent. *International Journal of Environmental Research*, 11(1), 91-98.
 23. Pashaei, S., Siddaramaiah, & Syed, A. A. (2011). Investigation on mechanical, thermal and morphological behaviors of turmeric spent incorporated vinyl ester green composites. *Polymer-Plastics Technology and Engineering*, 50(12), 1187-1198.
 24. Razia S, Taqui SN, Zameer F, Usman SN, Syed AA. (2017). Adsorption of ethidium bromide from aqueous solution on to nutraceutical industrial fennel seed spent: Kinetics and thermodynamics modeling Studies. doi-10.1080/15226514.2017.1365331.
 25. Syed, M. A., & Syed, A. A. (2016). Investigation on physicomechanical and wear properties of new green thermoplastic composites. *Polymer Composites*, 37(8), 2306-2312.
 26. Syed, M. A., & Syed, A. A. (2016a). Development of green thermoplastic composites from Centella spent and study of its physicomechanical, tribological, and morphological characteristics. *Journal of Thermoplastic Composite Materials*, 29(9), 1297-1311.
 27. Syed, M. A., & Syed, A. A. (2012). Development of a new inexpensive green thermoplastic composite and evaluation of its physico-mechanical and wear properties. *Materials & Design* (1980-2015), 36, 421-427.
 28. Syed, M. A., Akhtar, S., & Syed, A. A. (2011). Studies on the physico-mechanical, thermal, and morphological behaviors of high density polyethylene/coleus spent green composites. *Journal of Applied Polymer Science*, 119(4), 1889-1895.
 29. Syed, M. A., Ramaraj, B., Akhtar, S., & Syed, A. A. (2010). Development of environmentally friendly high density polyethylene and turmeric spent composites: Physicomechanical, thermal, and morphological studies. *Journal of Applied Polymer Science*, 118(2), 1204-1210.
 30. Syed, M. A., Siddaramaiah, Syed, R. T., & Syed, A. A. (2010a). Investigation on physico-mechanical properties, water, thermal and chemical ageing of unsaturated polyester/turmeric spent composites. *Polymer-Plastics Technology and Engineering*, 49(6), 555-559.
 31. Syed, M. A., Siddaramaiah, Suresha, B., & Syed, A. A. (2009). Mechanical and abrasive wear behavior of coleus spent filled unsaturated polyester/polymethyl methacrylate semi interpenetrating polymer network

- composites. *Journal of Composite Materials*, 43(21), 2387-2400.
32. Taqui, S. N., Yahya, R., Hassan, A., Nayak, N., & Syed, A. A. (2017). Development of sustainable dye adsorption system using nutraceutical industrial fennel seed spent-studies using Congo red dye. *International Journal of Phytoremediation*, 19(7), 686-694.
33. Velmurugan, P., Kumar, R. V., & Dhinakaran, G. (2011). Dye removal from aqueous solution using low cost adsorbent. *International Journal of Environmental Sciences*, 1(7), 1492.
34. www.prnewswire.com, 2015.
35. Zhang, H., Tang, Y., Cai, D., Liu, X., Wang, X., Huang, Q., & Yu, Z. (2010). Hexavalent chromium removal from aqueous solution by algal bloom residue derived activated carbon: equilibrium and kinetic studies. *Journal of Hazardous Materials*, 181(1), 801-808.
36. Zhang, H., Tang, Y., Liu, X., Ke, Z., Su, X., Cai, D., & Yu, Z. (2011). Improved adsorptive capacity of pine wood decayed by fungi *Poria cocos* for removal of malachite green from aqueous solutions. *Desalination*, 274(1), 97-104.

How to cite this article:

Razia Sulthana and Akheel Ahmed Syed. 2018, A Design For Sustainable Technology And Adsorption Studies on Removal of Malachite Green From Water Using Nutraceutical Industrial Fennel Seed Spent. *Int J Recent Sci Res.* 9(2), pp. 23953-23963. DOI: <http://dx.doi.org/10.24327/ijrsr.2018.0902.1569>
